# Study of the Reduction and Reoxidation of a CaO Surface

**Filip Acke\* and Itai Panas**

*Department of Inorganic Chemistry, Chalmers University of Technology and Göteborg University,*
*S-412 96 Göteborg, Sweden*

**Dan Strömberg**

*Department of Applied Environmental Science, Göteborg University, Medicinaregatan 20 A,*
*S-413 90 Göteborg, Sweden*

The reduction of NO with CO and $H_2$ is shown to comprise two basic reactions: a surface oxygen abstraction by the reducing agent and a reoxidation of the surface by NO. The former reaction step has been demonstrated by transient $CO_2$ formation during CO exposure of oxidized CaO surfaces, while the latter was demonstrated by $N_2$ and/or $N_2O$ transient formation during NO exposure of a prereduced CaO surface. It was shown that at low temperatures (between room temperature and 500 °C) both $N_2$ and $N_2O$ were formed, but at temperatures above 500 °C only $N_2$ was observed. The activation energies of the respective steps have been determined using temperature-programmed reaction experiments. The activation energy of the surface oxygen abstraction was determined to be 25 kcal/mol and is similar to the apparent activation energy of the overall reaction. The activation energy of the NO bond breakage was determined to be maximum 10 kcal/mol as measured by $N_2O$ formation. The importance of an $N_2O_2^-$ or $N_2O_2^{2-}$ intermediate in the formation of $N_2O$ will be discussed, and the importance of $N_2O$ decomposition in forming $N_2$ at temperatures above 500 °C will be compared with a N surface diffusion mechanism.

## I. Introduction

Mechanistic studies of the reduction of NO over noble-metal surfaces such as well-defined Rh{110}[1] have led to an understanding, resulting in an improved design of three-way catalysts used for car exhaust cleaning. A drawback of some of these catalysts is the formation of $N_2O$ during NO reduction.[2] The $N_2O$ formation after NO adsorption on well-characterized metal surfaces has been studied, and two possible mechanisms have been suggested. Dissociative adsorption of NO has been supported for Cu{100},[3,4] Cu{111},[5] and W{110}[6] surfaces, while for an Ag{111} surface a mechanism based on the formation of an $(NO)_2$ dimer has been proposed.[7] The activation energy of the formation of adsorbed $N_2O$ from $(NO)_2$ dimers on Ag{111} has been determined to be 7.3 kJ/mol. Behm and Brundle monitored the desorption peaks of $N_2O$ over the same surface and found $N_2O$ desorption at 124, 220, and 415 K.[8] In the presence of Na, Goddard et al.[9] observed at 300 K a strongly bound NO state that reacted to form $N_2$, $N_2O$, and $O_2$.

For other applications, such as electric utilities, other much cheaper solutions are sought. Zhang et al.[10] examined the selectivity and activity of Li-promoted MgO materials toward the reduction of NO by methane. NO reduction activity was observed for temperatures over 500 °C. At this temperature both $N_2$ and $N_2O$ were found as reaction products. Increasing the temperature resulted in an increased selectivity toward the $N_2$ formation. As contrasted with the mechanistic understanding of the $N_2O$ formation over well-defined metal surfaces, such as Ag, Cu, and W surfaces, the understanding of the $N_2$ and $N_2O$ formation over Li-promoted MgO surfaces is not well-known.

This article is part of a series that tries to elucidate the nitrogen chemistry during NO reduction over alkaline-earth oxides. In previous work,[11] the reduction of NO with CO and $H_2$ has been investigated over different CaO materials. Similar apparent activation energies for the overall reactions of NO reduction with $H_2$ and CO (when corrected for $CO_2$ poisoning) were found for all investigated materials. It was also observed that different impurity concentrations did not significantly affect the apparent activation energy but that the preexponential factor, when related to the surface area, increased with increasing impurity concentration. A two-step reaction model was then proposed based on a surface reduction step (pointed out as the rate-limiting one), followed by a surface reoxidation step. The activity of $CH_4$ as a reducing agent was also investigated, but an increase of the apparent activation energy for NO reduction indicated a more complex reaction mechanism.

In this article, the catalytic activity of a CaO surface toward the NO reduction with $H_2$ and CO will be examined more in detail by separating the surface oxygen abstraction and the surface reoxidation step. The activation energy for the surface oxygen abstraction step is determined by means of temperature-programmed reaction experiments. NO reoxidates the surface, and the final reaction products are found to depend on temperature. At low temperatures $N_2O$ and $N_2$ are formed while at elevated temperatures only an $N_2$ production is found. The temperature-programmed reaction technique is also employed to determine the apparent activation energy for $N_2O$ formation which can be considered to give an upper limit for the activation energy of the N−O bond breakage. Based on the low- and high-temperature reoxidation results in combination with the absence of $O_2$ formation during the reoxidation, $N_2O_2^-$ or $N_2O_2^{2-}$ will be suggested to be the important intermediate species in the NO reduction over alkaline-earth oxide surfaces.

## II. Experimental Section

A fixed bed quartz reactor connected to a quadropole mass spectrometer (QMG 421 of Balzers) was used for the experi-

\* Corresponding author: tel +46 (0)31 772 28 86; fax +46 (0)31 772 28 53; e-mail filip@inoc.chalmers.se.

Reduction and Reoxidation of a CaO Surface

*J. Phys. Chem. B, Vol. 101, No. 33, 1997* **6485**
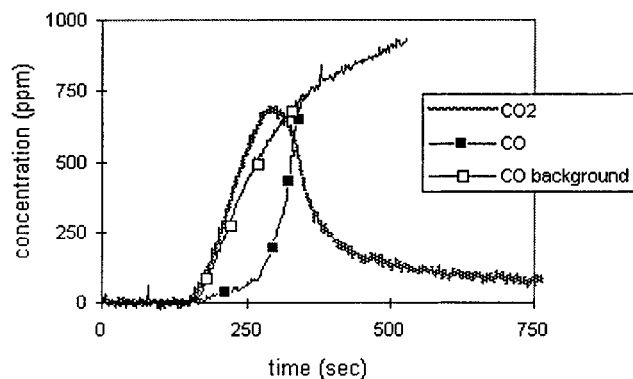


**Figure 1.** Transient $CO_2$ production and CO concentration during exposure of a bed containing 0.5636 g of CaO mixed with 1.7500 g of $SiO_2$ to a gas flow of CO mixed with Ar at 800 °C.

ments. The quartz reactor had an inner diameter of 22 mm, a length of 500 mm, and an asymmetric construction to avoid heating of the upper metal fitting and the vacuum-tight Viton O-ring. The gas sampling was done 2 mm under the bed supporting sintered quartz filter, by a quartz capillary.[12] The temperature was measured with a K-type thermocouple 3 mm under the capillary tip, avoiding interference of catalytic reactions on the thermocouple. The heating ramps were controlled with a second K-type thermocouple in contact with the heating coil and connected to a Eurotherm temperature controller leading to very linear heating ramps.

The bed materials consisted of a mixture of CaO (Fisher Scientific) with quartz sand, pro analysi (Merck), to reduce the pressure drop. The gases used were 5000 ppm NO, CO, and $H_2$ in Ar. The gases were mixed with pure Ar, and the flows were controlled by mass flow controllers (Brooks, Type 5850 E) to a total flow of about 25 mL/min at 1 atm and 293 K. All gases were delivered by AGA. One experiment was performed with isotope-labeled $^{15}NO$ to be able to separate $N_2$ and CO and $N_2O$ and $CO_2$.

### III. Results

**III.1. Surface Oxygen Abstraction: $CO_2$ Production.** A CaO surface was first exposed for 15 min at 800 °C in a gas flow of 27 mL/min containing about 900 ppm NO in Ar to fully oxidize the CaO surface. The bed material was then exposed to a gas mixture of about 1000 ppm CO in Ar, total gas flow of 22.7 mL/min, at 650 and 800 °C for about 20 min. Initially, no CO was detected in the gas mixture; instead, a transient $CO_2$ production could be observed (Figure 1). The surface was subsequently reoxidized by NO at 800 °C. The same reaction was also studied over quartz sand. It is known that quartz sand is relatively inactive toward the NO reduction with CO at these temperatures.[13] No transient $CO_2$ production was detected, but instead the CO signal was found to shift to faster responding times (Figure 1). The CO signal for the bed consisting of quartz sand is referred to as the "CO background" in the figure.

In order to obtain a further understanding of the transient $CO_2$ production, a series of bed materials were tested in which the amount of CaO was doubled, tripled, and finally quadrupled. The $CO_2$ production was measured for two temperatures, 650 and 800 °C. In Figure 2 ((a) 650 and (b) 800 °C) the transient $CO_2$ productions are shown, and correlation is observed between the amount of CaO in the bed and $CO_2$ peak intensity. Increase in the amount of CaO in the bed results in an increased $CO_2$ production. Although a significant spread can be observed on the amount of produced $CO_2$, a trend following the ratio series 2, 3, and 4 cannot be denied. It can also be observed that when
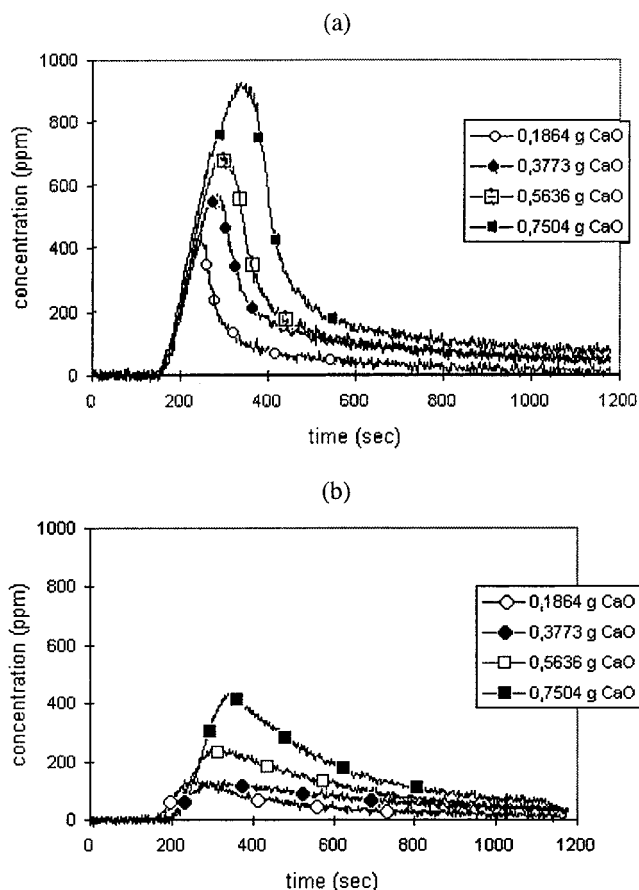


**Figure 2.** Influence of the amount of CaO in the bed on the transient $CO_2$ production at (a) 800 and (b) 650 °C.

the temperature of reduction is increased, the height of the $CO_2$ peak also increases.

A complication, in evaluating the data comprised in the Figures 1 and 2, is found in the extensive $CO_2$ tail. The tail results from minor oxygen impurities in the respective gases. When the $CO_2$ production is calculated by integrating under the $CO_2$ curve, correction is made for these tails. It has been found to be impossible to reproduce the $CO_2$ transient effect once the CaO-containing bed has been exposed to a reducing gas flow. Instead, the tail value is obtained. Only after surface reoxidation and subsequent CO exposure can a $CO_2$ transient be observed. It is concluded that the only route to $CO_2$ formation is via a surface oxygen abstraction step.

**III.2. Surface Reoxidation: $N_2$ and $N_2O$ Production.** Different types of reoxidation experiments have been performed. The first one, *high-temperature reoxidation*, consisted of the reoxidation of a CO reduced surface with NO at the temperature of reduction (650 and 800 °C). A second set of experiments, *low-temperature reoxidation*, consisted of the reoxidation of an 800 °C prereduced surface by NO adsorption at room temperature followed by a temperature ramp to 800 °C in Ar and a final NO exposure at 800 °C to obtain a complete reoxidized surface. In a last set of experiments the temperature dependence of the surface oxygen abstraction step was investigated. Two types of experiments were set up. In a first series of experiments, the temperature of CO exposure was varied between 500 and 850 °C, while the surface after each reduction was reoxidized at 800 °C with NO. A second series of experiments combined a comparison between CO and $H_2$ as reducing agents and the effect of temperature on the surface reduction. A fully oxidized surface was reduced in a CO or $H_2$ atmosphere at temperatures between 450 and 800 °C and reoxidized with NO
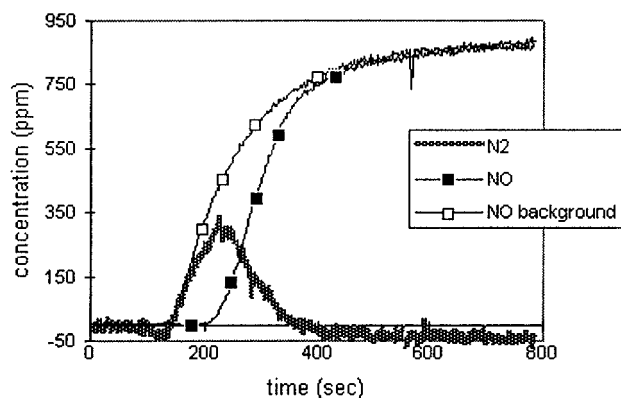
**Figure 3.** Transient $N_2$ production and NO concentration during exposure of a prereduced (800 °C) bed containing 0.5636 g of CaO mixed with 1.7500 g of $SiO_2$ to a gas flow of NO mixed with Ar at 800 °C.

at room temperature followed by a temperature ramp up to 800 °C in Ar monitoring the $N_2$ and $N_2O$ production. Again, the surface was exposed to NO at 800 °C to ensure that all the sites created during the reduction step were reoxidized before a new experiment was started.

*III.2.1. High-Temperature Reoxidation.* Exposing at 800 °C a prereduced CaO surface, prereduced at 800 °C, to about 900 ppm NO in Ar results in a transient $N_2$ formation as shown in Figure 3. This transient can be compared to the one of the surface oxygen abstraction step, shown as a $CO_2$ transient in Figure 1. Comparing the $N_2$ and NO signals, it can be observed that first all NO is reduced to $N_2$, while the NO signal is delayed in time. The transient $N_2$ peak disappears when a bed of only quartz sand is tested. At the same time, it can be observed that the NO response time is shorter for quartz sand. This is expected, keeping in mind the analogy with the surface oxygen abstraction step. In Figure 3, the NO signal for the bed material of quartz sand is referred to as "NO background".

The amount of CaO in the bed was doubled, tripled, and quadrupled, as was done for the $CO_2$ production. This was done to ensure that the observed $N_2$ production is not an artifact and related to the presence of CaO in the reactor. An increase in $N_2$ production, following the ratio series 2, 3, and 4, can be observed in Figure 4 ((a) for 650 and (b) 800 °C). This behavior correlates with that shown in Figure 2 for the $CO_2$ production during the reduction step. To avoid any confusion, it might be a good idea to summarize the chronology of the experiments. First, the fresh bed was exposed to NO at 800 °C in order to fully oxidize the surface. Then the bed was exposed to CO at 800 °C, and a $CO_2$ formation was observed. This prereduced surface was exposed to NO at 800 °C, and the $N_2$ formation was monitored. Then the temperature was lowered to 650 °C in an Ar atmosphere, and the surface reduction and reoxidation cycle was repeated at this temperature. Finally, the temperature of the bed material was increased to 800 °C in Ar, and the bed was then exposed to NO in order to reobtain the initial surface.

These experiments show that the NO + CO overall reaction can be divided into two more basic reactions: a reducing step followed by an oxidizing step. The surface oxygen abstraction leaves electrons in the substrate and creates sites for the NO dissociation. This results, at elevated temperatures, in an $N_2$ production and a reoxidation of the surface. In all these experiments no other possible reaction products, such as $N_2O$ and $NO_2$, have been detected.

*III.2.2. Low-Temperature Reoxidation.* Exposure at room temperature of an 800 °C prereduced bed to NO leads to the formation of $N_2$ and $N_2O$ as is shown in Figure 5a. The



(a)



(b)
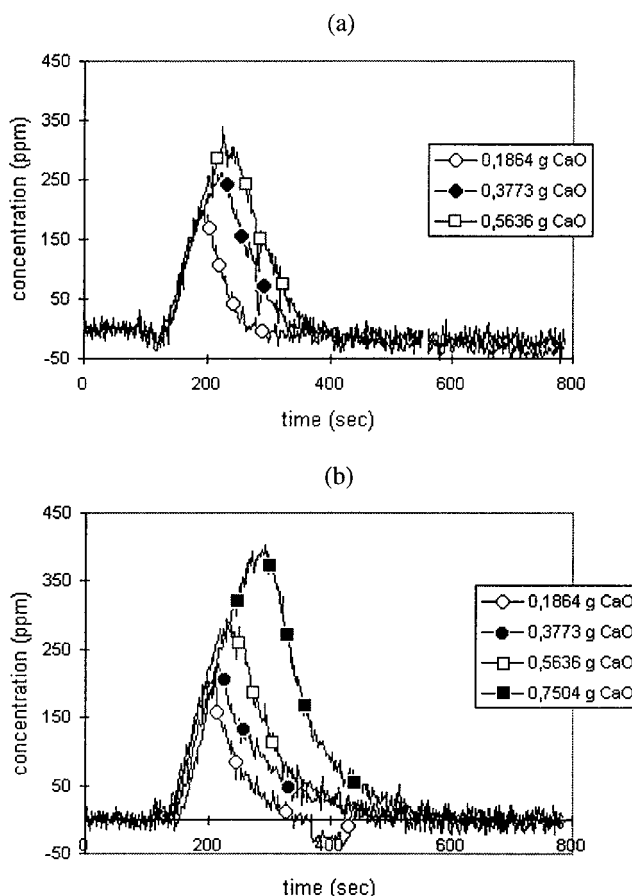
**Figure 4.** Influence of the amount of CaO in the bed on the transient $N_2$ production at (a) 800 and (b) 650 °C.

observed transient $N_2$ peak is due to a reaction channel for complete reduction of NO. The $N_2$ formation is accompanied by the partial reduction of NO to $N_2O$ as shown in the figure. After some time, the room temperature reduction capacity of the reduced CaO bed diminishes, and the $N_2$ and $N_2O$ signals decline. Attention should be drawn on the chronological order of the NO and $N_2O$ peaks. The appearance of the $N_2O$ when the $N_2$ peak has started to decline could indicate that the $N_2$ formation is a result of the decomposition of an $N_2O$ intermediate species.

Subsequently, the bed was heated to 800 °C in Ar while measuring the respective $N_2$, $N_2O$, and NO concentrations. The results are displayed in Figure 5b. Two NO desorption peaks can be observed. At 139 °C an $N_2O$ peak is observed, while at higher temperatures two $N_2$ peaks appear. In this figure, the change in $N_2$ signal is not so pronounced, but experiments with an increased heating rate leave no doubt about the $N_2$ formation. Finally at 800 °C, the bed was reexposed to NO (the same gas mixture as in the beginning of the experiment). A transient $N_2$ formation could be observed (Figure 5c), demonstrating that not all sites are reoxidized during the previous treatment. To ensure that the observed species at masses 28 and 44 are $N_2$ and $N_2O$, respectively, the same experiment has been redone with isotope-labeled $^{15}NO$. Similar curves are obtained, but now on mass 30 and 46 as expected.

The fact that NO can be reduced to form $N_2$ and $N_2O$ at temperatures as low as room temperature has important consequences. It indicates a similarity in product formation between well-defined metal surfaces, such as Ag{111} with or without the presence of Na (see Introduction), and prereduced CaO surfaces for the temperature interval investigated here. The absence of an $O_2$ desorption during all previous experiments is

Reduction and Reoxidation of a CaO Surface

*J. Phys. Chem. B, Vol. 101, No. 33, 1997* **6487**

(a)



(b)



(c)
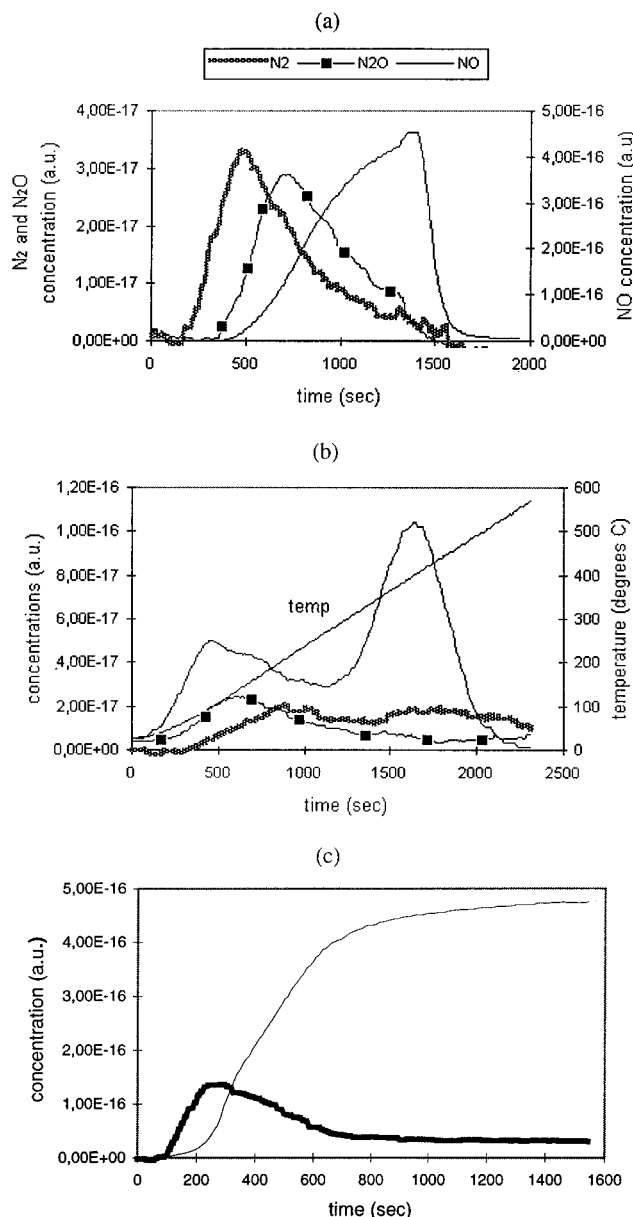


**Figure 5.** (a) Transient $N_2$ and $N_2O$ production of a prereduced (800 °C) bed containting 0.75 g of CaO mixed with 1.75 g of $SiO_2$ to a gas flow of NO mixed with Ar at room temperature. (b) Transient $N_2$ and $N_2O$ production and NO desorption during a heating ramp of 0.25 K/s between room temperature and 550 °C in an Ar gas flow. (c) Transient $N_2$ production at 800 °C when the previously treated surface is exposed to NO, final surface reoxidation.

in line with a reoxidation of the CaO surface. The low temperatures at which this nitrogen chemistry is observed indicate that the apparent activation energies for these reactions leading to the formation of $N_2$ and $N_2O$ must be low. On the other hand, the surface oxygen abstraction needs a temperature of at least about 500 °C. This temperature is comparable with the temperature for NO reduction with methane as published by Zhang et al.[10] This suggests that the surface oxygen abstraction could be the rate-limiting step. This will be proven later by determining the kinetics of the respective steps (see below).

Possible qualitative influences on $N_2$ and $N_2O$ formation were investigated (i) by varying the exposure time to NO, at room temperature, for an 800 °C prereduced surface and (ii) by varying the exposure time to CO at 800 °C for a fully oxidized surface. This prereduced surface was then cooled in Ar to room temperature and reoxidized by NO. To check the former one

(i), the surface was initially exposed to the reducing agent for 20 min at 800 °C. After cooling in Ar to room temperature, the reduced surface was exposed to NO. This sequence was repeated for different NO exposure times (5, 15, and 30 min). No significant difference in the $N_2$ and $N_2O$ formation was observed. In the latter experiments (ii), the influence of the reducing time on the $N_2$, and $N_2O$ formation was checked by exposing the substrate for 40 min to CO instead of 20 min. Again, no significant difference in the $N_2$ and $N_2O$ formation was observed. This indicates that all sites are created after 20 min of exposure to the reducing agent.

*III.2.3. Influence of Reducing Temperature on the Oxygen Abstraction Step.* The temperature dependence of the surface oxygen abstraction step was examined in more detail. A fully oxidized bed material was therefore exposed to CO at different temperatures between 500 and 850 °C monitoring the transient $CO_2$ formation. The respective surface oxygen abstractions were then followed by a change in temperature to 800 °C in an Ar atmosphere, still measuring any possible $CO_2$ production. At 800 °C, the surface was reoxidized with NO, and the transient $N_2$ formation was followed. The advantage of reoxidizing the surface at a constant temperature is found in the elimination of possible temperature effects in the NO reduction and $N_2$ formation mechanism. In Figure 6a the sum of the $CO_2$ produced at the respective reduction temperatures and the amount of $CO_2$ that is formed or that desorbs during heating between reduction temperature and reoxidation temperature (800 °C) is shown. The latter $CO_2$ contribution was only observed for surface oxygen abstraction between 500 and 700 °C. This temperature interval is in agreement with the thermodynamic stability of carbonates. In Figure 6a, it can be seen that the $CO_2$ production, and thus the oxygen abstraction reaction, decreases with decreasing temperature. At 500 °C, no direct surface oxygen abstraction can be observed. However, during heating up some $CO_2$ is observed leading to the production of active sites as was shown by the $N_2$ formation during reoxidation. Two possible configurations can be thought of: a bridged CO between two neighboring $O^{2-}$ species or a carbonate readsorbed on the surface after a surface oxygen abstraction. The former would lead to the formation of a $CO_2$ during heating up, while the latter would lead to the desorption of $CO_2$. A plateau in the $CO_2$ curve between 550 and 650 °C can be observed. This plateau is the result of an increasing $CO_2$ production with increasing reduction temperature combined with a decreasing $CO_2$ production or desorption during heating when the reduction temperature is increased.

The $N_2$ production at 800 °C for the respective reducing experiments is shown in Figure 6b. A behavior different from the above is observed. The formation of $N_2$ stays constant for the experiments where the reduction step is performed in a temperature interval between 600 and 850 °C. For temperatures lower than 600 °C, the $N_2$ formation declines. At the plateau level, the $N_2$ to $CO_2$ ratio is approximately one. This suggests that each produced site by a surface oxygen abstraction by CO results in the formation of one $N_2$ molecule. However, at temperatures above about 650 °C, this ratio decreases to about half suggesting the formation of one $N_2$ for two formed $CO_2$ molecules.

A similar result is obtained for the sum of the $N_2O$ and $N_2$ formation when the surface is reoxidized with NO at room temperature after the materials have been reduced at temperatures between 450 and 800 °C. In Figure 7, the sum of the produced amounts of $N_2$ and $N_2O$, normalized to that produced for a surface oxygen abstraction step with CO at 800 °C, is shown as a function of the surface oxygen abstraction temper-

(a)



(b)



(c)
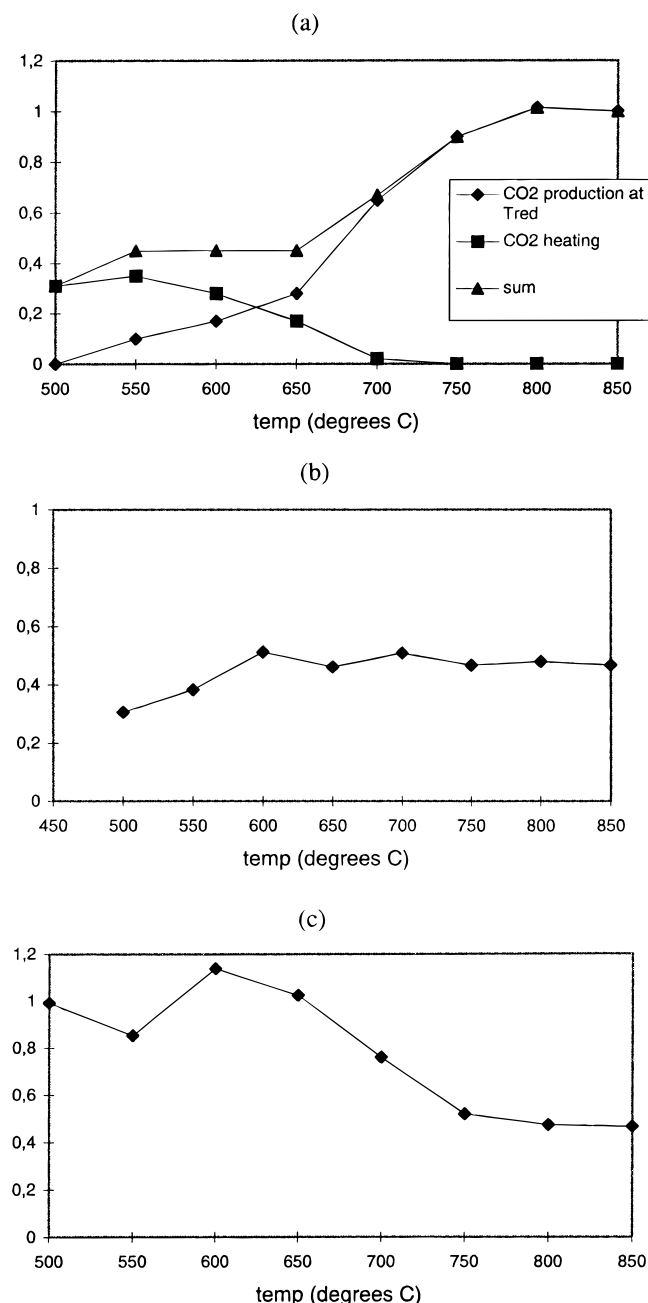


**Figure 6.** (a) Ratio between transient $CO_2$ production at different reduction temperatures and the transient $CO_2$ production at 800 °C plotted versus the reduction temperature. (b) Corresponding $N_2$ production (related to the $N_2$ production at 800 °C) at 800 °C (c) $N_2/CO_2$ ratio.

ature for both CO and $H_2$ as reducing agent. An increasing ratio with increasing temperature is observed until about 600 °C where the sum of the $N_2$ and $N_2O$ production becomes almost constant. No significant difference between CO and $H_2$ as reducing agent is observed. This is in agreement with previous results[11] where no difference in apparent activation energy was found for the NO + CO and the NO + $H_2$ overall reactions.

**III.3. Kinetics.** Equations relating Arrhenius kinetical parameters $A$ and $E_a$ (preexponential factor and apparent activation energy, respectively), surface coverage $\theta$, and linear heating rate $\beta$ have been reviewed by Lord and Kittelberger.[14] It was shown that the slope of a plot of $\ln(T_m^2\theta_m^{n-1}/\beta)$ versus $1/T_m$ reproduces the apparent activation energy for desorption in which $T_m$ stands for the peak temperature, $\theta_m$ for the peak coverage, and $n$ for the order of desorption. In this work, the order $n$ will be taken as one, which simplifies the plot to ln-
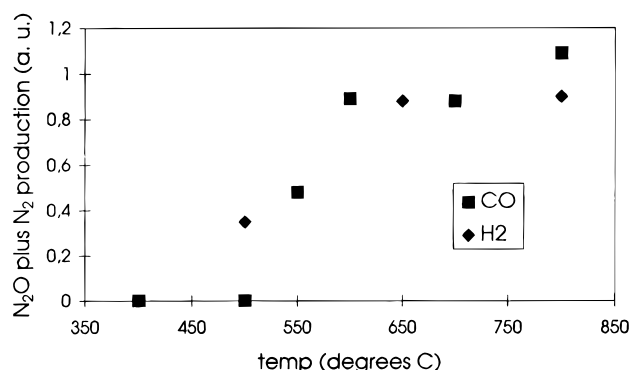


**Figure 7.** $N_2O + N_2$ production as a function of the reduction temperature for $H_2$ and CO as reducing agent (related to the sum of the $N_2$ and $N_2O$ production at 800 °C).
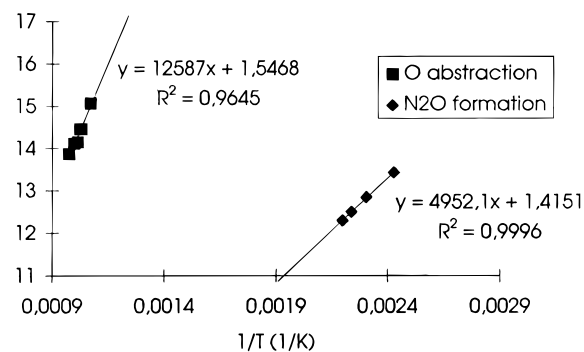


**Figure 8.** Activation energy determination of the surface oxygen abstraction step and the reoxidation of the surface.
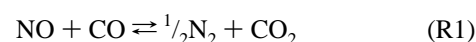
$(T_m^2/\beta)$ versus $1/T_m$. Calculations have shown that assuming a reaction order of 1 does not introduce a major mistake in the case the order is in reality higher than one.[14]

By plotting $\ln(T_m^2/\beta)$ versus $1/T_m$ (Figure 8), we determined the activation energies of the surface oxygen abstraction and a maximum of the surface reoxidation to be about 25 and 10 kcal/mol respectively. The former was determined by exposing a fully reoxidized surface to CO at room temperature for 15 min followed by a heating ramp in Ar, with well-defined heating rates, measuring the temperature of maximum $CO_2$ evolution. For the latter, an 800 °C prereduced surface was exposed to NO at room temperature followed by a heating ramp as previously discussed and shown in Figure 5b for the $N_2O$ evolution.
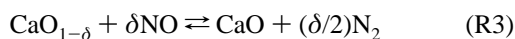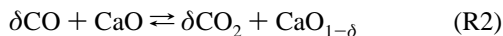
**IV. Discussion**

In a previous work,[11] it was shown that the catalytic activity of CaO surfaces toward NO reduction depends on the impurity content of the material. It was demonstrated that an increased impurity content has the effect to increase the preexponential factor, but not to affect the apparent activation energy of the reaction. The effect of $Ca^{2+}$ substitution by $Na^+$ ions for the oxidative coupling of methane has been shown by Lin et al.,[15] while both Ito et al.[16,17] and Coulter et al.[18−20] examined the activity of the related Li-doped MgO system toward this reaction. Electron paramagnetic resonance experiments demonstrated the appearance of $O^-$ species in this type of doped system,[15,21,22] and the importance of these $O^-$ species in the catalytic activity of these materials has been suggested.[15−18,20]

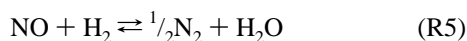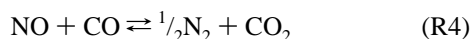The results in the present study show that the overall reaction

$$NO + CO \rightleftharpoons {}^1\!/_2N_2 + CO_2 \qquad (R1)$$

can be divided into two more basic reactions:

$$\delta CO + CaO \rightleftharpoons \delta CO_2 + CaO_{1-\delta} \qquad (R2)$$

$$CaO_{1-\delta} + \delta NO \rightleftharpoons CaO + (\delta/2)N_2 \qquad (R3)$$

where $\delta$ is a number related to the number and type of impurities.

The apparent activation energy of the overall reactions

$$NO + CO \rightleftharpoons {}^1/_2 N_2 + CO_2 \qquad (R4)$$

$$NO + H_2 \rightleftharpoons {}^1/_2 N_2 + H_2O \qquad (R5)$$

catalyzed by different CaO surfaces has been determined to be between 26 and 27 kcal/mol, independent of the type of CaO material.[11] Comparison of this value with the apparent activation energies for surface oxygen abstraction and $N_2O$ formation, as determined by temperature-programmed reaction experiments produced in the present study, suggests the surface oxygen abstraction to be the rate-limiting step in the overall reaction mechanism.

Two possible interpretations of the roles of $O^-$ species on the surface oxygen abstraction step have been proposed: one based on a semiconductor model[15] and one based on a localized picturel.[20] The two scenarios were discussed in more detail in a previous work.[11] In this discussion more attention will be given to the reoxidation of the surface. It has been shown that in a temperature interval between room temperature and approximately 500 °C, depending on heating rate, NO is first fully and then partially reduced, forming $N_2$ and $N_2O$, respectively. At higher temperatures, no $N_2O$ was detected, suggesting a complete reduction of NO to $N_2$. Two reaction paths can be proposed for the formation of $N_2$: (i) one based on $N_2O_2^-$ and/or $N_2O_2^{2-}$ and (ii) a second one based on surface diffusion of atomic N.

The first scenario assumes the formation of $N_2O_2^-$ and/or $N_2O_2^{2-}$ intermediate species. Breaking an N–O bond in these dimers leads to the formation of an $N_2O$ intermediate (R6) and a reoxidation of the CaO surface (R7).

$$2NO + CaO_{1-\delta} \rightleftharpoons \delta N_2O_{2(ads)} + CaO_{1-\delta} \qquad (R6)$$

$$\delta N_2O_{2(ads)} + CaO_{1-\delta} \rightleftharpoons \delta N_2O + CaO \qquad (R7)$$
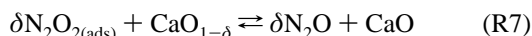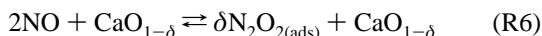
The formation of the anionic intermediates on CaO surfaces reminds of the $(NO)_2$ dimers described by Brown et al.[7] for Ag {111} surfaces at much lower temperatures (70–90 K). For these surfaces the NO dimer decomposes to form an adsorbed oxygen and an $N_2O$ molecule. A similar mechanism has been discussed by Platero et al.[23] for $N_2O$ formation during NO adsorption on MgO surfaces between 77 K and room temperature. The important intermediate in this reaction was suggested to be an $N_2O_2^{2-}$ ion, which dissociates to an $N_2O$ molecule and an ionic crystal oxygen. Surface $N_2O_2^{2-}$ species have also been observed by Cerruti et al.[24] by means of infrared spectroscopy.
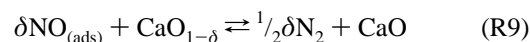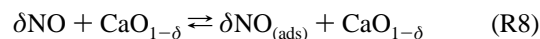
The $N_2O$ decomposition to $N_2$ is catalyzed further both by reduced and unreduced CaO surfaces. The chronology in the $N_2$ and $N_2O$ formation, as shown in Figure 5a, indicates that a reduced CaO surface is still active toward $N_2O$ decomposition at room temperature. The $N_2O$ decomposition over a prereduced CaO surface results in reoxidation of the surface. However, over an unreduced CaO surface, a temperature of at least 500 °C is needed for $N_2O$ decomposition.[25] Over these surfaces the $N_2O$ decomposition results in the formation of peroxide

**TABLE 1: Approximate $N_2/CO_2$ Ratio for the Different Reaction Mechanisms**

| | $N_2O$ decomposition: fate of the extra O | | | |
|---|---|---|---|---|
| | N surface diffusion | $O_2$ desorption | excess O removal | filling up the reactive site |
| $N_2/CO_2$-ratio | $^1/_2$ | 1 | $^1/_2$ | $^1/_2$ |

ions.[26] These peroxide ions are removed either by oxygen recombination and desorption[27] or by a reducing agent.[28]

The second scenario toward $N_2$ formation is based on atomic nitrogen surface diffusion, followed by an N–N recombination step:

$$\delta NO + CaO_{1-\delta} \rightleftharpoons \delta NO_{(ads)} + CaO_{1-\delta} \qquad (R8)$$

$$\delta NO_{(ads)} + CaO_{1-\delta} \rightleftharpoons {}^1/_2 \delta N_2 + CaO \qquad (R9)$$

No kinetical data are available for the surface diffusion and recombination of atomic nitrogen over CaO surfaces. However, the data obtained by Nakamura et al.[29] for the oxygen diffusion, 44 kcal/mol for the apparent activation energy for the surface diffusion and recombination of oxygen at low oxygen coverages, combined with the absence of any oxygen evolution during the present experiments makes the N–N recombination mechanism less likely.

In Figure 6c the experimentally observed ratio between $N_2$ formation and the corresponding $CO_2$ formation is shown. For temperatures up to about 650 °C a plateau is observed where this ratio is about one. Above this temperature the ratio decreases to become approximately one half at 800 °C and stays rather constant up to 850 °C. In Table 1, it is suggested that the only mechanism resulting in a ratio of 1 is the one due to $O_2$ desorption, but as pointed out previously, no $O_2$ desorption has been observed. Hence, a mechanism explaining this temperature dependence is still open for discussion and is left for further investigations.

## V. Conclusions

The reduction of NO with CO and $H_2$ is shown to comprise two more basic reactions: a surface oxygen abstraction and a reoxidation of the surface. The former reaction step has been demonstrated by transient $CO_2$ formation during CO exposure of oxidized CaO surfaces, while the latter was demonstrated by $N_2$ and/or $N_2O$ transient formation during NO exposure of a prereduced CaO surface. The low-temperature (between room temperature and 500 °C) $N_2O$ formation suggests the importance of $N_2O_2^-$ or $N_2O_2^{2-}$ species in the NO reduction. The absence of $N_2O$ for temperatures over 500 °C has been discussed in relation to the fast $N_2O$ decomposition over CaO surfaces, resulting in peroxide formation. The temperature dependence of the $N_2/CO_2$ ratio is not yet understood.

The activation energies of the respective steps have been determined using temperature-programmed reaction experiments. The activation energy of the surface oxygen abstraction step was determined to be 25 kcal/mol and is similar to the apparent activation energy of the overall reaction, making the surface oxygen abstraction step the rate-determining one in the overall reaction mechanism. The activation energy of the NO bond breakage was determined to be maximum 10 kcal/mol as measured by $N_2O$ formation.

**References and Notes**

(1) Baraldi, A.; Dhanak, V. R.; Gomelli, G.; Kiskinova, M.; Rosei, R. *Appl. Surf. Sci.* **1993**, *68*, 395.

Acke et al.

(2) Nieuwenhuys, B. E.; Siera, J.; Tanaka, K.-I.; Hirano, H. *Environ. Catal.* **1994**, 114.

(3) Wendelken, J. F. *Appl. Surf. Sci.* **1982**, *11/12*, 172.

(4) Johnson, D. W.; Matloob, M. H.; Roberts, M. W. *J. Chem. Soc., Chem. Commun.* **1978**, 40.

(5) Johnson, D. W.; Matloob, M. H.; Roberts, M. W. *J. Chem. Soc., Faraday Trans. 1* **1979**, *75*, 2143.

(6) Masel, R. I.; Umbach, E.; Fuggle, J. C.; Menzel, D. *Surf. Sci.* **1979**, *79*, 26.

(7) Brown, W. A.; Gardner, P.; King, D. A. *J. Phys. Chem.* **1995**, *99*, 7065.

(8) Behm, R. J.; Brundle, C. R. *J. Vac. Sci. Technol.* **1984**, *A3*, 1040.

(9) Goddard, P. J.; West, J.; Lambert, R. M. *Surf. Sci.* **1978**, *71*, 447.

(10) Zhang, X.; Walters, A. B.; Vannice, M. B. *J. Catal.* **1994**, *146*, 568.

(11) Acke, F.; Panas, I.; Strömberg, D. Submitted to *J. Catal.*

(12) Kasemo, B. *Rev. Sci. Instrum.* **1979**, *50*, 1602.

(13) Olanders, B.; Strömberg, D. *Energy Fuels* **1995**, *9*, 680.

(14) Lord, F. M.; Kittelberger, J. S. *Surf. Sci.* **1974**, *43*, 173.

(15) Lin, C.-H.; Wang, J.-X.; Lunsford, J. H. *J. Catal.* **1988**, *111*, 302.

(16) Ito, T.; Lunsford, J. H. *Nature* **1985**, *314*, 721.

(17) Ito, T.; Wang, J.-X.; Lin, C. H.; Lunsford, J. H. *J. Am. Chem. Soc.* **1985**, *107*, 5062.

(18) Coulter, K.; Goodman, D. W. *Catal. Lett.* **1992**, *16*, 191.

(19) Coulter, K.; Goodman, D. W. *Catal. Lett.* **1992**, *20*, 169.

(20) Wu, M.-C.; Truong, C. M.; Coulter, K.; Goodman, D. W. *J. Catal.* **1993**, *140*, 344.

(21) Tohver, H. T.; Henderson, B.; Chen, Y.; Abraham, M. M. *Phys. Rev. B* **1972**, *5*, 3276.

(22) Abraham, M. M.; Chen, Y.; Boatner, L. A.; Reynolds, R. W. *Phys. Rev. B* **1976**, *37*, 3276.

(23) Platero, E. E.; Spoto, G.; Zecchina, A. *J. Chem. Soc., Faraday Trans. 1* **1985**, *81*, 1283.

(24) Cerruti, L.; Modone, E.; Guglielminotti, E.; Borello, E. *J. Chem. Soc., Faraday Trans. 1* **1974**, *70*, 729.

(25) Miettinen, H.; Strömberg, D.; Lindqvist, O. *Proceedings of the 11th International Conference on Fluidized Bed Combustion*; ASME: New York, 1991; p 1027.

(26) Snis, A.; Strömberg, D.; Panas, I. *Surf. Sci.* **1993**, *292*, 317.

(27) Snis, A.; Panas, I. *J. Chem. Phys.* **1995**, *103*, 7626.

(28) Snis, A.; Panas, I.; Strömberg, D. *Surf. Sci.* **1994**, *310*, L579.

(29) Nakamura, M.; Mitsuhashi, H.; Takezawa, N. *J. Catal.* **1992**, *138*, 686.